THE ASTROPHYSICAL JOURNAL, 494:822–827, 1998 February 20

ON THE OUTGASSING PROFILE OF COMET HALE-BOPP

K. R. FLAMMER,[1] D. A. MENDIS,[1] AND H. L. F. HOUPIS[2]
Received 1997 June 20; accepted 1997 September 24

ABSTRACT

When Comet Hale-Bopp was first discovered at a heliocentric distance of ~7.2 AU, its activity appeared to be controlled by the outgassing of the highly volatile CO molecule. Its gas production remained CO-driven until about 4 AU when the outgassing became controlled by the less volatile H_2O molecule. While the outgassing around this distance is consistent with the sublimation from a large "dirty snowball" composed dominantly of H_2O, the subsequent outgassing at smaller heliocentric distance up to perihelion ($d \approx 0.914$ AU) falls consistently below the predictions of such a model. In this paper, we use the earliest chemical differentiation model of the cometary nucleus developed by Houpis et al., with a few modifications, to show that the continuous chemical differentiation of a deepening layer of the cometary nucleus which has made multiple passages into the inner solar system can explain comet Hale-Bopp's observed pre-perihelion production rate curve. It also predicts a hysteresis with the gas production rate profiles falling systematically lower post-perihelion. The model suggests that comet Hale-Bopp is a complex combination of dust, clathrate, and volatile (mainly CO), the gas production of which changes from being CO-driven to H_2O driven around 4 AU. Furthermore, the thermal insulation provided by a growing dust mantle inside ~3.5 AU causes the H_2O production rate curve to flatten-out.

Subject headings: comets: individual (Hale-Bopp) — molecular processes

1. INTRODUCTION

Comet Hale-Bopp was discovered at a heliocentric distance ~7.2 AU (Offutt 1995). Its activity at these large heliocentric distances appeared to be controlled by the outgassing of the highly volatile molecule CO (Matthews, Jewitt, & Senay 1995; Jewitt, Senay, & Matthews 1996; Rauer et al. 1995; Biver et al. 1996a, 1996b). The situation changed near 4 AU when the outgassing was controlled by the less volatile H_2O molecule (D. Jewitt 1997, private communication) which is generally regarded to be the dominant volatile species in the cometary nucleus (e.g., Delsemme 1982). While the outgassing around this distance is consistent with the sublimation from a large "dirty snowball" composed dominantly of H_2O, the subsequent outgassing at smaller heliocentric distances up to perihelion ($r \approx 0.914$ AU) falls consistently below the predictions of such a model.

In this paper we show that the continuous chemical differentiation of a deepening layer of the cometary nucleus (assumed to be initially chemically homogeneous) could explain both these observations. The basic model is described in § 2, the results of the model are presented in § 3, followed by a discussion in § 4.

The distant activity of this comet has been explained by Prialnik (1997) on the basis of crystallization of an initially amorphous ice nucleus leading to the release of occluded gases such as CO. Orbital evolution calculations of comet Hale-Bopp (Bailey et al. 1996) indicate that this comet is not dynamically new in the sense of coming "fresh" from the Oort cloud. Consequently we consider it more appropriate to assume that the water ice, at least in the upper part of the comet, is in a crystalline form.

[1] Department of Electrical and Computer Engineering, University of California, San Diego, La Jolla, CA 92093.
[2] Astronomy Department, Sierra College, Rocklin, CA 95677.

2. THE MODEL

The model used here is essentially the earliest chemical differentiation model of the nucleus developed by Houpis, Ip, & Mendis (1985) with a few modifications. As in this earlier model, we consider the thermal evolution of a nucleus initially composed of a homogeneous grainy admixture of dust, H_2O-clathrate grains, and grains of another ice more volatile than the clathrate. In this earlier model Houpis et al. (1985) assumed this volatile ice to be CO_2. Since we now know that the early activity of comet Hale-Bopp was controlled by CO rather than CO_2, we will use CO as the volatile ice in the nucleus of our comet model rather than CO_2.

We emphasize that the model we are considering, namely the admixture of grains of different chemical composition is consistent with the planetesimal accretion model for the formation of solar system bodies (e.g., Safranov 1972; Alfvén & Arrhenius 1976). We also note that some chemical species more volatile than H_2O, including CO, can be trapped in the clathrate lattice, and so will be emitted together with H_2O. However, only a maximum of one such guest molecule per six H_2O molecules is possible. Any constituent with a higher abundance than that will be present as a separate ice, mixed with the clathrate ice and dust.

A schematic of the physical model is shown in Figure 1. After a time t, the undifferentiated core of dust, clathrate, and CO-ice will be surrounded by two mantles, the lower one, Δ_i, being evacuated of CO and the upper one, Δ_o, evacuated of both CO and clathrate. Our treatment is one dimensional since both Δ_o and Δ_i are much smaller the nuclear radius, R_n. We also assume that the mantle development is quasi-stationary since the characteristic time for heat to be conducted to the core is much less than the characteristic time for orbital change.

The basic equations governing the development of the mantles are given in Houpis et al. (1985). Here we repeat them, with the appropriate minor changes, for complete-

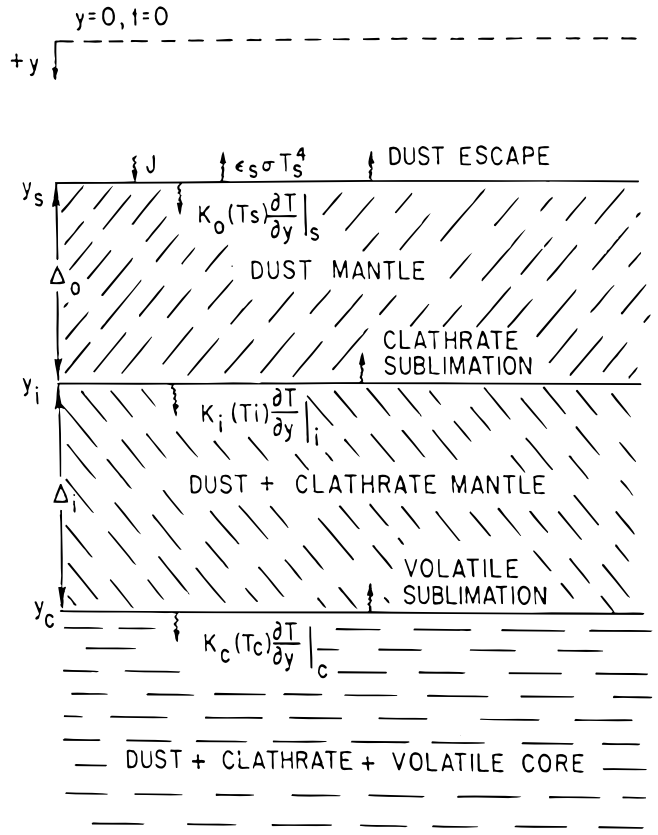

FIG. 1.—Schematic diagram of a chemically differentiated nucleus showing the energy balance used at the three interfaces y_s, y_i, and y_c; $y = 0$, $t = 0$. The outer mantle, the dust mantle, has a thickness Δ_o', the inner mantle, composed of dust and clathrate, has a thickness Δ_i (Houpis et al. 1985).

ness. They are:

$$\dot{\Delta}_i = \dot{y}_c - \dot{y}_i = \frac{f_v m_v}{g_v \rho_v} \dot{Z}_v(T_c) - \frac{f_{\rm cl} m_{\rm cl}}{g_{\rm cl} \rho_{\rm cl}} \dot{Z}_{\rm cl}(T_i) , \quad (1)$$

and

$$\dot{\Delta}_o = \dot{y}_i - \dot{y}_s = \frac{f_{\rm cl} m_{\rm cl}}{g_{\rm cl} \rho_{\rm cl}} \dot{Z}_{\rm cl}(T_i) - \frac{\beta_d}{g_d \rho_d} \times [(\gamma_{\rm cl} m_{\rm cl} k T_i)^{1/2} f_{\rm cl} \dot{Z}_{\rm cl}(T_i) + (\gamma_v m_v k T_c)^{1/2} f_v \dot{Z}_v(T_c)] . \quad (2)$$

Here the suffixes v, cl, and d denote the volatile (CO), the clathrate, and the dust, respectively, while g and f represent the volume and surface fractions of the respective components with

$$g_v = \frac{\chi_v/\rho_v}{\chi_v/\rho_v + \chi_{\rm cl}/\rho_{\rm cl} + \chi_d/\rho_d} ,$$

and $f_v = g_v^{2/3}$ (and similar expressions for $g_{\rm cl}$, g_d, and $f_{\rm cl}$ and f_d), with χ and ρ denoting the mass fractions and the mass densities. We also take $m_{\rm cl} = \frac{6}{7} m_{\rm H_2O} + \frac{1}{7} \bar{m}_g$ (where $\bar{m}_g$ is the average mass of all the guest molecules trapped in the clathrate. The sublimation rate $\dot{Z}$ ($\rm cm^{-2}\ s^{-1}$) occurring in the above equations are calculated from the Clausius-Clapeyron equation and are given by

$$\dot{Z}_{\rm cl}(T_i) = n_{o,\rm cl} \left(\frac{\gamma_{\rm cl} k T_i}{m_{\rm cl}} \right)^{1/2} \frac{T_{o,\rm cl}}{T_i} \exp \left[\frac{b_{\rm cl}}{N_A k} \left(\frac{1}{T_{o,\rm cl}} - \frac{1}{T_i} \right) \right] , \quad (3)$$

and

$$\dot{Z}_v(T_c) = n_{o,v} \left(\frac{\gamma_v k T_c}{m_v} \right)^{1/2} \left(\frac{T_{o,v}}{T_c} \right)^{1 - m/N_A k} \times \exp \left[\frac{b_v}{N_A k} \left(\frac{1}{T_{o,v}} - \frac{1}{T_c} \right) \right] . \quad (4)$$

Here γ is the ratio of specific heats, with $\gamma_{\rm cl} = \frac{1}{7}\bar{\gamma}_g + \frac{6}{7}\gamma_{\rm H_2O}$. The parameters $n_{o,\rm cl}$, $T_{o,\rm cl}$, $b_{\rm cl}$, $n_{o,v}$, T_{ov} b_v (with v replaced by CO), and m are given in Table 1, together with the values of all the other parameters used in the model.

The second term appearing in equation (2) represents the rate at which dust is "blown-off" the upper surface and following the core-mantle model of Horanyi et al. (1984), it is assumed that it is proportional to the total gas momentum flux from the surface with β_d being the proportionality factor.

Equations (1) and (2) constitute two independent model equations in the five unknowns: Δ_i, Δ_o, T_c, T_i, and T_s. We require three more independent equations to complete the set of model equations. These are the energy balance equations at each of the three surfaces (s, i, and c). The energy balance at the outer surface is

$$\frac{1 - A_s}{d^2} J = \epsilon_s \sigma T_s^4 - K_o(T) \nabla T |_s , \quad (5)$$

where A_s is the surface Albedo, $\epsilon (= 1 - A_s)$ is the emissivity, J is the average solar constant over the surface of the nucleus [$= (1.4 \times 10^6)/4$ ergs $\rm cm^{-2}\ s^{-1}$], d is the helio-

TABLE 1

MODEL PARAMETERS

Parameter	Value
A_s	0.8 (no mantle) → 0.025 (with mantle)
e	0.995108
a	186.82 AU
χ_v	0.05
χ_d	0.50
$\chi_{\rm cl}$	0.45
$m_{\rm H_2O}$	3.006×10^{-23} g
$n_{o,\rm cl}$	1.94×10^{19} $\rm cm^{-3}$
$T_{o,\rm cl}$	393 K
$\gamma_{\rm H_2O}$	1.33
$b_{\rm cl}$	5×10^{11} ergs $\rm mol^{-1}$
α	1.0×10^{-4} cm
$K_{\rm bo}$	6×10^5 ergs $\rm cm^{-1}$
ρ_v	1 g $\rm cm^{-3}$
ρ_d	2 g $\rm cm^{-3}$
$\rho_{\rm cl}$	1 g $\rm cm^{-3}$
$m_{\rm CO}$	4.67×10^{-23} g
$n_{o,\rm CO}$	4.414×10^{18} $\rm cm^{-3}$
$T_{o,\rm CO}$	61.55 K
$\gamma_{\rm CO}$	1.4
$b_{\rm CO}$	1.0496×10^{11} ergs $\rm mol^{-1}$
m	-3.6949×10^8 ergs $\rm mol^{-1}\ K^{-1}$
$K_{\rm bi}$	6×10^6 ergs $\rm cm^{-1}\ K^{-1}\ s^{-1}$
l_o	4.4×10^{-5} cm
l_i	2.3×10^{-4} cm
β_d	3×10^{-5}

centric distance in AU, and K_o is the thermal conductivity of the dust mantle. For the dust layer,

$$-K_o(T)\nabla T|_s = f_{\rm cl}\frac{L_{\rm cl}}{N_A}\dot{Z}_{\rm cl}(T_i) - K_i(T)\nabla T|_i\,, \qquad (6)$$

and for the clathrate layer,

$$-K_i(T)\nabla T|_i = f_v\frac{L_v}{N_A}\dot{Z}_v(T_c) + f_{\rm cl}\frac{L_{\rm cl}}{N_A}\dot{Z}_{\rm cl}(T_c)\,, \qquad (7)$$

where K_i is the thermal conductivity of the inner mantle and $L_{\rm cl}$ and L_v are the latent heats of vaporization of the clathrate and volatile respectively.

While the first of these equations expresses the fact that all the solar energy reaching the upper surface is either reradiated back into space or conducted through the mantle, the last express the assumption that all the energy reaching the core is entirely utilized in sublimating its surface.

Assuming that there are no sources or sinks for the heat flow in the mantles [i.e., $-K(T)\nabla T = \text{constant}$] we get

$$-K_o(T)\nabla T|_s = \frac{1}{\Delta_o(d)}\int_{T_i}^{T_s}K_o(T)dT = [\alpha K_{bo}(T_s - T_i) + \sigma\epsilon_s l_o(T_s^4 - T_i^4)]/\Delta_o(d)\,, \qquad (8)$$

and

$$-K_i(T)\nabla T|_i = \frac{1}{\Delta_i(d)}\int_{T_c}^{T_i}K_i(T)dT = [\alpha K_{bi}(T_i - T_c) + \sigma\epsilon_s l_i(T_i^4 - T_c^4)]/\Delta_i(d)\,. \qquad (9)$$

Here we have assumed that the thermal conductivity can be written in the form (see Brin & Mendis 1979)

$$K(T) = \alpha K_b + 4\sigma\epsilon_s l T^3\,, \qquad (10)$$

where K_b is the bulk conductivity of the mantle material, α is the Hertz factor, and l is the average intergrain distance in the mantle.

In order to use the heliocentric distance, d, rather than the time t as the independent variable we need the relation between t and d, which, assuming that the comet travels in an elliptical orbit around the Sun, is (see Kaula 1968),

$$t - t_0 = (GM_S)^{-1/2}a^{3/2}\left\{\arccos\left[\frac{1}{e}\left(1 - \frac{d}{a}\right)\right] - e\sin\arccos\left[\frac{1}{e}\left(1 - \frac{d}{a}\right)\right]\right\}, \qquad (11)$$

where a and e are, respectively, the semi-major axis and the eccentricity, t_o is the time of perihelion passage, and M_S is the solar mass.

Equations (1), (2), (5), (6), (7) together with the subsidary equations (3), (4), (8), (9), and (11), form the complete set of model equations for the calculation of Δ_o, Δ_i, T_s, T_i, and T_c [together with $\dot{Z}_{\rm cl}(T_i)$ and $\dot{Z}_v(T_c)$] as a function of d.

In their calculations, Houpis et al. (1985) assumed the same albedo for the surface of the nucleus, both when it had a dust mantle and when it did not. This is unrealistic because the dust covered surface could be quite dark, as was observed at comet Halley (e.g., see Mendis et al. 1989), while the undifferentiated icy surface would have a much higher albedo. Here we also take this into consideration by allowing the surface albedo to change as it develops a dust mantle.

3. RESULTS

The early observations of comet Hale-Bopp, when it was 6–7 AU from the Sun, indicated that this comet was excessively bright due to substantial sublimation of CO (Biver et al. 1996a; Jewitt et al. 1996). Additionally, Sekanina (1996) concluded that Hale-Bopp was extremely dust-rich. CO production continued to increase as Hale-Bopp approached the Sun and even at 4.6 AU, CO sublimation dominated over H_2O (Crovisier et al. 1996). Close to 4 AU, H_2O sublimation took over as the primary source of activity in comet Hale-Bopp (D. Jewitt 1997, private communication). While the CO production flattened out inside this heliocentric distance, the production of H_2O increased steadily until Hale-Bopp's perihelion at 0.914 AU, although not as rapidly as predicted by our earlier model assuming an undifferentiated, slowly rotating, purely H_2O nucleus (Flammer, Mendis, & Shapiro 1997). The present model, allowing for the gradual chemical differentiation of the outer layer of an initially homogeneous nucleus as it orbits the Sun, is used to explain the observed CO and H_2O production rates at comet Hale-Bopp, including the heliocentric distance where the outgassing activity changed from CO-dominated to H_2O-dominated. Since comet Hale-Bopp is unlikely to be a new comet coming freshly from the Oort cloud (Bailey et al. 1996), we consider the effects of multiple passages of the Sun on the gas production rate profiles.

Table 1 lists the values used to obtain the results discussed below. The values of $n_{o,\rm cl}$, $T_{o,\rm cl}$, and $b_{\rm cl}$ are standard in the literature, while those of $n_{o,\rm CO}$, $T_{o,\rm CO}$, $b_{o,\rm CO}$, and m are those used by Houpis & Mendis (1981). The thermal conductivity of the mantles are taken from Brin & Mendis (1979). Expressions for the intergrain spacings, l_o and l_i, are given in Houpis et al. (1985).

Initially the chemically homogeneous comet nucleus has a composition (by mass) of 45% clathrate, 50% dust, and 5% CO. A medium value of the dust proportionality parameter, $\beta_d = 3 \times 10^{-5}$ is used for our modeling purposes (e.g., see Houpis et al. 1985). We also assume that the clathrate is occupied by 5% CO, the remaining 10% accounting for all other species trapped in the clathrate. Since we do not know the composition of all these species, we take $\bar{m}_g \approx m_{\rm CO}$ and $\bar{\gamma}_g \approx \gamma_{\rm CO}$.

To integrate the system of equations (1), (2), (5), (6), and (7), we start at a large heliocentric distance (75 AU) beyond which CO sublimation is negligible (e.g., Delsemme 1982). At this heliocentric distance, on the first orbit,

$$\Delta_{o,\rm initial}(\text{orbit} = 1) = \Delta_{i,\rm initial}(\text{orbit} = 1) = 0\,,$$

and

$$T_s = T_i = T_c = (J/d^2\sigma)^{1/4} \approx 30\ \text{K}\,.$$

For each orbit the system of equations is integrated from this initial distance to perihelion and then back to this point. (Again, the rationale being that from $\sim$75 AU to aphelion the CO gas production is negligible). However, on each successive orbit the final values of Δ_i and Δ_o from the previous orbit are used for the initial conditions, i.e.,

$$\Delta_{i,\rm initial}(\text{orbit} = n) = \Delta_{i,\rm final}(\text{orbit} = n - 1)\,,$$

$$\Delta_{o,\rm initial}(\text{orbit} = n) = \Delta_{o,\rm final}(\text{orbit} = n - 1)\,.$$

When the integration begins at a large heliocentric distance for the initial orbit, the comet is highly reflective due to the presence of ice at the surface and thus we assume an albedo of 0.8. As a dust mantle develops, the albedo is reduced (proportional to the dust mantle thickness) to 0.025. Such limits are chosen based on observational evidence: the first one is compatible with the albedo measured for icy satellites in the solar system, while the second one is similar to measured albedo of comet Halley at perihelion when it was almost completely covered with dust.

Our calculations were performed for multiple orbits. While the outer and inner mantles increase significantly from their first-orbit values, orbit to orbit, the temperature profiles show very little change. With each passage of the Sun, the gas production weakens as the mantles grow. However the relative change in the production rate profiles decreases with each new orbit and by the tenth orbit, the production rate profiles are almost independent of orbit number. For this reason we have only shown orbit 10, which is representative of all later orbits. As the conglomerate nucleus approaches the Sun during the first orbit, the CO ice on the surface begins to sublimate at quite large heliocentric distances ($d \sim 70$ AU), leading to a steady growth of the clathrate mantle: Δ_i reaches 3 cm at 70 AU, 120 cm at 50 AU, 275 cm at 25 AU, and 428 cm at 1 AU. By the 10th orbit, the clathrate mantle reaches $\sim$1900 cm (see Fig. 2). As the clathrate mantle grows, the temperature differential between the two surfaces, the core and the interface, T_c and T_i, increases, as shown in Figure 3. Initially, $T_c = T_i = 30$ K at 75 AU whereas $T_c \approx 32$ K and $T_i \approx 180$ at 1 AU. The volatile CO in the core nucleus continues to sublimate at the lower core temperature. The less volatile clathrate begins to sublimate at higher temperatures around 30 AU when $T_i \approx 58$ K. The total production rate of CO is given by

$$Q_{\rm CO} = \epsilon_{\rm cl} f_{\rm cl} \dot{Z}_{\rm cl}(T_i) + f_v \dot{Z}_v(T_c) , \qquad (12)$$

where $\epsilon_{\rm cl} = 0.05$ is the fraction of CO trapped in the clathrate. Throughout Hale-Bopp's approach to the Sun, the majority of CO production comes from the sublimating core, the second term on the right-hand side of the above equation, and a lesser amount from the clathrate mantle sublimation. For example even at 1 AU the ratio of the CO production rate from the core and the clathrate mantle is $\approx$1.88. As a result, the present observations, while being consistent with the clathrate model that we have adopted, cannot discriminate between it and one composed of pure crystalline H_2O ice. One may need to await an appropriate in situ measurement or even perhaps a sample return cometary mission before this question is finally resolved. As illustrated in Figure 3, the temperature of the core, T_c varies very little over Hale-Bopp's orbit which explains the relative constant production rate of CO discussed in the following section.

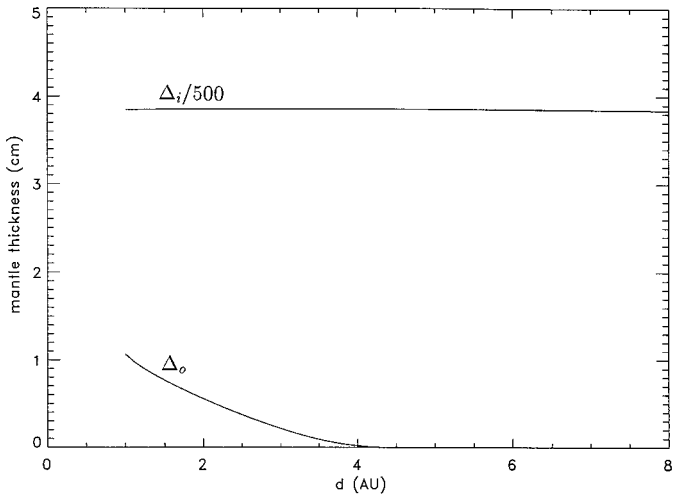

FIG. 2.—Variation of the inner and outer mantle thickness for Comet Hale-Bopp during its 10th orbit. The inner mantle is scaled by a factor of 500.

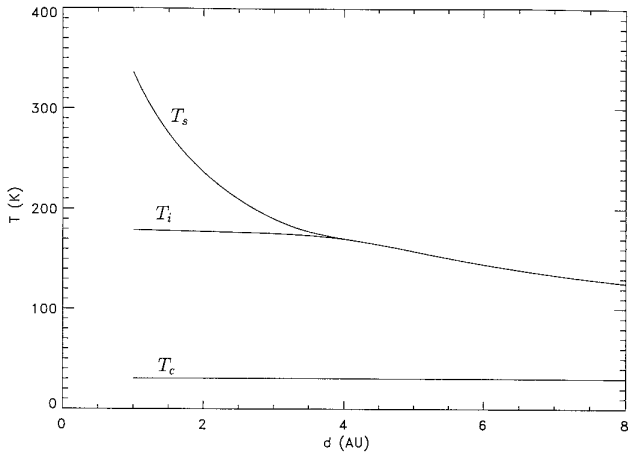

FIG. 3.—temperature profiles of the interface surfaces at comet Hale-Bopp during its 10th orbit.

The outer dust mantle on the other hand, does not develop until close to 3.5 AU, when the surface temperature, T_s, is about 175 K. Inside 3.5 AU, the dust mantle grows slowly until perihelion, reaching a thickness of $\sim$1 cm at 1 AU on the tenth orbit. The surface temperature of the nucleus keeps increasing to 335 K at 1 AU, whereas the interface temperature, T_i, remains fairly constant, reaching $\approx$180 K at 1 AU.

4. DISCUSSION AND CONCLUSION

The chemically differentiated nucleus model determines the sublimation rates $\dot{Z}_{\rm cl}$ and $\dot{Z}_v$ given in equations (3) and (4). The "corrected" H_2O and CO sublimation rates are given by

$$F_{\rm H_2O} = 6/7 f_{\rm cl} \dot{Z}_{\rm cl}(T_i) , \qquad (13)$$

and

$$F_{\rm CO} = \epsilon_{\rm cl} f_{\rm cl} Z_{\rm cl}(T_i) + f_v \dot{Z}_v(T_c) , \qquad (14)$$

respectively. An important consequence of the chemically differentiated nucleus is that the ratio of the H_2O production rate to that of CO given by,

$$R = \frac{F_{\rm H_2O}}{F_{\rm CO}} \qquad (15)$$

changes from being less than 1 to greater than 1 during the comet's orbit. At comet Hale-Bopp, this change in R (when $R \approx 1$) occurred around 4 AU.

The total production rate of each species is given by,

$$Q = A_{\rm eff} F_i = 4\pi R_{\rm eff}^2 F_i , \qquad (16)$$

where $R_{\rm eff}$ is the "effective" radius of the nucleus for sublimation and F_i are the sublimation rates of H_2O and CO given, respectively, by equations (13) and (14). The actual radius of the cometary nucleus R_n would be larger than $R_{\rm eff}$ if only a fraction f of the surface is active. The effective sublimation area, $A_{\rm eff}$ is adjusted so that the H_2O production rate determined by our model agrees with the observed H_2O production rate at 4.5 AU of 4.1×10^{28} mol s^{-1} (Weaver et al. 1996). This $A_{\rm eff}$ is then used to determine $Q_{\rm CO}$ using equations (14) and (16). The value of $A_{\rm eff}$ indicates that the radius of Hale-Bopp's nucleus is $\gtrsim 5$ km which is in reasonable agreement with the lower limit of the radius determined by Jewitt et al. (1996) using CO observations at 6.6 AU ($\approx$2–4 km).

Figure 4 shows the CO gas production rate (*dotted lines*; the upper curves corresponding to the first orbit and the lower ones to the tenth) and the H_2O production rate (*dash-dot-dot line* for the first orbit and *solid line* for the tenth orbit) determined by the chemically differentiated nucleus model. Also shown in this figure is our (Flammer et al. 1997) earlier calculation of Hale-Bopp's H_2O production rate where we assumed an undifferentiated, slowly rotating, pure H_2O nucleus (*dashed line*). The CO (*diamonds*) and H_2O (*asterisk*) determined from various pre-perihelion observations (referenced in Table 2) are also shown in Figure 4. By using a model which allows for the gradual chemical differentiation of the outer layer of the nucleus we obtain production rate profiles which agree remarkably well with the observed production rates of both CO and H_2O.

The H_2O and CO production rate profiles do not vary in the same manner throughout Hale-Bopp's orbit. The large variation in the H_2O production rate is correlated with the variation of Hale-Bopp's surface temperature, which increases rapidly as the comet approaches the Sun (see Fig. 3). Around 3.5 AU a dust mantle begins to form (see Fig. 2). After the dust mantle forms, the H_2O production rate increases less rapidly due to increasing thermal insulation

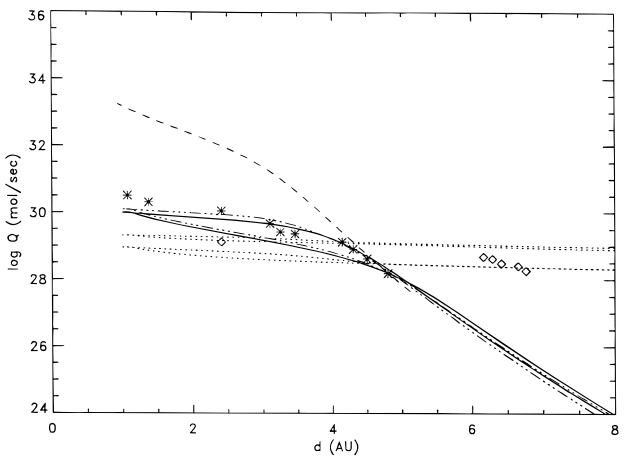

FIG. 4.—Production rate profiles for comet Hale-Bopp. Dashed curve assumes an undifferentiated slowly rotating, purely H_2O nucleus. Dash-dot-dot curve represents the H_2O production rate determined by the mantle nuclear model after the first orbit; solid curve represents the H_2O production rate determined by the mantle nuclear model after 10 orbits. Dotted curve represents the CO production rate determined by the mantle nuclear model. (The higher curve corresponds to the initial orbit; the lower curve corresponds to the tenth orbit). Asterisks indicate the preperihelion H_2O production rates determined from observations (given in Table 2). Diamonds indicate the preperihelion CO production rates determined from observations (also given in Table 2).

TABLE 2

H_2O AND CO OBSERVATIONS

d (AU)	Molecule	Q (s^{-1})	Reference
6.76	CO	1.8×10^{28}	1
6.649.....	CO	2.5×10^{28}	1
6.414.....	CO	3×10^{28}	1
6.290.....	CO	4.1×10^{28}	1
6.165.....	CO	4.7×10^{28}	1
2.41	CO	1.3×10^{29}	2
4.8	H_2O	1.5×10^{28}	3
4.5	H_2O	4.1×10^{28}	3
4.3	H_2O	8×10^{28}	4
4.14	H_2O	1.3×10^{29}	4
2.88	H_2O	4.7×10^{29}	2
2.41	H_2O	1.1×10^{30}	2
1.37	H_2O	2×10^{30}	5
1.07	H_2O	3.16×10^{30}	5

REFERENCES.—(1) Jewitt et al. 1996; (2) Bockelee-Morvan et al. 1996; (3) Weaver et al. 1996; (4) Crovisier et al. 1996; (5) Crovisier 1997, private communication.

produced by the growing dust layer. The observations clearly indicate a flattening out of the H_2O production inside about 3.5 AU. The CO production at comet Hale-Bopp remains relatively constant since CO outgasses mainly from the core which has a very small temperature variation over the orbit as shown in Figure 3.

The main point of the present paper is to illustrate that the production rate curve for comet Hale-Bopp can be explained by the mantled nature of a chemically differentiated cometary nucleus. The model suggests that comet Hale-Bopp is a complex combination of dust, clathrate, and volatile (mainly CO), the gas production of which changes from being CO-driven to H_2O-driven around 4 AU. Furthermore, the thermal insulation provided by a growing dust mantle inside $\sim$3.5 AU causes the H_2O production rate curve to flatten out.

Although comet Hale-Bopp's orbital period is on the order of thousands of years, it is most likely not a "new" comet and has made previous passages around the Sun (Bailey et al. 1996). The results described above assume that the comet nucleus is initially undifferentiated, without a dust or clathrate mantle, when the calculations begin for the first inbound orbit. The consequences of these initial conditions on the production rate profiles were examined by carrying out the calculations for 10 orbits, using the same orbital elements for each orbit. After 10 orbits, there was very little change in the H_2O and CO gas production rate curves and the heliocentric distance where H_2O production overtook CO production remained near 4 AU. These calculations did however reveal an asymmetry of the gas production about perihelion; the production rate being lower outbound than inbound at the same heliocentric distance. Similar findings were reported by Houpis et al. (1985) and Horanyi et al. (1984) and can be explained by the continued growth of the dust mantle before perihelion, followed by a total blowoff at relatively large distances post-perihelion (beyond $\sim$40 AU for orbit 10). There are insufficient post-perihelion observations reported at present to check this predicted asymmetry.

We also examined the effect of using a lower value of $\beta_d (\approx 10^{-6})$ in our model, meaning that less momentum is transferred to the dust. In this case, the comet builds up larger and larger mantles with each orbit which suppress

the H_2O and CO production at a given heliocentric distance. The comet becomes progressively less active each orbit and consequently the production rate profile loses its asymmetry after many orbits. Such a comet will also have to be much larger than the present estimates for the size of comet Hale-Bopp.

The results of our chemical differentiation model are also sensitive to the assumed composition of the comet nucleus. The mass fractions adopted in the present discussion, i.e., $\chi_d = 0.50$, $\chi_{cl} = 0.45$, $\chi_{CO} = 0.05$, and the fraction of CO in the clathrate, where adjusted until the heliocentric distance where H_2O production overtook CO production agreed with observations (4 AU), while also reproducing the observed H_2O and CO production curves reasonably well. Increasing the mass fraction of CO in the nucleus moves the cross-over point to smaller heliocentric distances, whereas reducing the amount of CO (and increasing the amount of clathrate) moves this cross-over point to larger heliocentric distances.

A more refined chemical differentiation model should also take into account additional effects, such as the loss of heat within the mantles due to the diffusing gas (e.g., Horanyi et al. 1984), recondensation of the volatiles (e.g., Espinasse et al. 1991), and the effects of dust particles of different sizes (e.g., Orosei et al. 1995). If the comet is considered to be a new comet, one would also have to take into account the exothermic phase transition from amorphous to crystalline ice (i.e., Prialnik 1992). However, even with these modifications, which we plan to include in the future, the important consequences of the results presented here should still apply. In particular, we expect the mantled, chemically differentiated cometary nucleus to be driven by the volatile production at large heliocentric distances and then become H_2O dominated closer to the Sun. Furthermore, as the mantle thickness increases and the gas production is suppressed, the activity of the comet will be modified over its orbit.

We also note that further validation of our model awaits observations of Hale-Bopp's production rate postperihelion when we predict values slightly lower than the corresponding pre-perihelion measurements.

K. R. F. and D. A. M. acknowledge support from NASA grant NAGW 4264. H. L. F. H. acknowledges Independent Study support from EnviroSens, Inc. The authors are grateful to D. Jewitt for constructive criticisms and suggestions for improvement of an earlier version of this paper.

REFERENCES

Alfvén, H., & Arrhenius, G. 1976, NASA SP-345
Bailey, M. E., Emelyanenko, V. V., Hahn, G., Harris, N. W., Hughes, K. A., Muinonen, K., & Scotti, J. V. 1996, MNRAS, 281, 916
Biver, N., et al. 1996a, Nature, 380, 137
Biver, N., et al. 1996b, IAU Circ. 6421
Bockelee-Morvan, D., et al. 1996, IAU Circ. 6511
Brin, G. D., & Mendis, D. A. 1979, ApJ, 229, 402
Crovisier, T. Y. 1997,
Crovisier, T. Y., et al. 1996, A&A, 315, L385
Delsemme, A. H. 1982, in Comets, ed. L. L. Wilkening (Tucson: Univ. Arizona Press), 85
Espinasse, S., Klinger, J., Ritz, C., & Schmitt, B. 1991, Icarus, 92, 350
Flammer, K. R., Mendis, D. A., & Shapiro, V. D. 1997, ApJ, 482
Horanyi, M., Gombosi, T. I., Cravens, T. E., Korosmezey, A., Kecskemety, A., Nagy, A. F., & Szego, K. 1984, ApJ, 278, 449
Houpis, H. L. F., Ip, W.-H., & Mendis, D. A. 1985, AJ., 295, 654
Houpis, H. L. F., & Mendis, D. A. 1981, Moon Planets, 25, 95
Jewitt, D., Senay, M., & Matthews, H. 1996, Science, 271, 1110
Kaula, W. M. 1968, An Introduction to Planetary Physics: The Terrestrial Planets (New York: Wiley)
Matthews, H. E., Jewitt, D., & Senay, M. C. 1995, IAU Circ. No. 6234
Mendis, D. A., et al. 1989, Ann. Geophys., 7, 99
Offutt, W. 1995, IAU Circ. No. 6194
Orosei, R., et al. 1995, A&A, 301, 613
Prialnik, D. 1997, ApJ, 478, L107
———. 1992, ApJ, 388, 196
Rauer, H., et al. 1995, IAU Circ. No. 6236
Safronov, V. S. 1972, Evolution of the Protoplanetary Cloud and the Formation of the Earth and the Planets, trans. from Russian by the Israel Program for Scientific Translation (Jerusalem: Keter Press)
Sekanina, Z. 1996, A&A, 314, 957
Weaver, H. A., Feldman, P. D., A'Hearn, M. F., Arpigny, C., Brandt, J. C., & Randall, C. E. 1996, IAU Circ. No. 6376